Guiding Optical Light in Air Using an All-Dielectric Structure

Yoel Fink, Daniel J. Ripin, Shanhui Fan, Chiping Chen, John D. Joannopoulos, and Edwin L. Thomas

***Abstract*—The emergence of a dielectric omnidirectional multilayer structure [1]–[4] opens new opportunities for low loss broad-band guiding of light in air. We demonstrate the effectiveness of such an approach by fabricating a broad-band, low-loss hollow waveguide in the 10-μm region and measuring its transmission around a 90° bend. The generality of the solution enables the application of the method to many wavelengths of interest important in telecommunication applications as well as for guiding high-power lasers in medical and other fields of use.**

***Index Terms*— Dielectric, high-power lasers, hollow waveguides, light conduits, low-loss broad-band transmission, medical lasers, multimode waveguide, omnidirectional reflectors, optical fibers, optical confinement, single-mode waveguide.**

I. Introduction

GUIDING light in dielectric fibers has had a tremendous impact on many aspects of our life—we rely on fiber optics for communications as well as for illumination and a host of medical applications. The typical optical fiber has a high index core and a low index cladding such that the light is confined to the core by total internal reflection. Two inherent drawbacks exist in this approach: the first is absorption. Since the light is traveling through a dense medium for long distances, material absorption becomes significant even in low loss materials. To compensate for losses the fiber is doped with erbium which is used to amplify the signal. This in turn limits the bandwidth of the fiber to that of the narrow erbium excitation lines. The other weakness follows from the confinement mechanism—total internal reflection which confines light only of a limited angle. Conventional optical fibers cannot guide light around sharp turns, which is especially important in optical integrated circuits. Light guided in a hollow waveguide lined with an omnidirectional reflecting film propagates primarily through air and will therefore have substantially lower absorption losses. In addition, the confinement mechanism does not have angular dependence allowing for guiding light around sharp bends with little or no leakage.

Most hollow waveguides fabricated to date [5]–[7], have internal metallic and dielectric layers. It has been shown [8] that the addition of dielectric layers to a metallic waveguide could lower the losses significantly. In contrast, our system is an all dielectric waveguide which confines all frequencies contained in its omnidirectional range. In principle this type of structure can have lower losses than the combined metal and dielectric structure since the waves do not interact with a lossy metallic layer. Although our proof of concept demonstration involves a large diameter multimode waveguide, one can fabricate a much smaller tube that could in principle be made to support a single mode.

II. Principle of Operation

A schematic of the hollow tube is presented in Fig. 1, as well as the index of refraction profile. In a realistic light guiding scenario involving many bends there exist no global symmetries and thus one cannot distinguish between independent TE and TM modes. Locally one can define a plane of incidence with respect to the normal to the film surface and the incident wave vector. Light entering into such a tube will invariably hit the walls many times and explore a wide range of angle of incidence of both polarizations with respect to any local plane of incidence. Since the air region is bounded by a structure that has a gap which encompasses all angles and polarizations the wave will be reflected back into the tube and will propagate along the hollow core as long as $k_z \neq 0$.

III. Sample Preparation Procedure

A Drummond 1.92 mm o.d. silica glass capillary tube was cleaned in concentrated sulfuric acid. The first tellurium layer was thermally evaporated using a LADD 30 000 evaporator fitted with a Sycon Instruments STM100 film thickness monitor. The capillary tube was axially rotated to ensure uniformity during coating. The first polymer layer was deposited by dip coating the capillary tube in a solution of 5.7 g polystyrene DOW 615APR in 90 g toluene. The next layer is tellurium deposited in the same method outlined above. The subsequent polymer layers are made of polyurethane diluted in mineral spirits. The device has a total of nine layers, five Te and four polymer and a total length of 10 cm. The layer thickness are approximately 0.8 μm for the tellurium layer (refractive index 4.6) and 1.6 μm for the polystyrene layer (refractive index 1.59). An optimal design will vary the layer thickness according to the zeros of the Bessel functions. Performance as

Manuscript received August 13, 1999. This work was supported in part by the Defense Advanced Research Agency through the U.S. Army Research Office under Grant DAAG55-97-1-0366 and by the Air Force Office of Scientific Research under Grants F49620-97-1-0325 and F49620-97-1-0385.

Y. Fink is with the Department of Materials Science and the Plasma Science and Fusion Center, Massachusetts Institute of Technology, Cambridge, MA 02139 USA (e-mail: yoel@mit.edu).

D. J. Ripin, S. Fan, and J. D. Joannopoulos are with the Department of Physics, Massachusetts Institute of Technology, Cambridge, MA 02139 USA (e-mail: shanhfan@mit.edu).

C. Chen is with the Plasma Science and Fusion Center, Massachusetts Institute of Technology, Cambridge, MA 02139 USA.

E. L. Thomas is with the Department of Materials Science, Massachusetts Institute of Technology, Cambridge, MA 02139 USA (e-mail: elt@mit.edu).

Publisher Item Identifier S 0733-8724(99)08813-1.

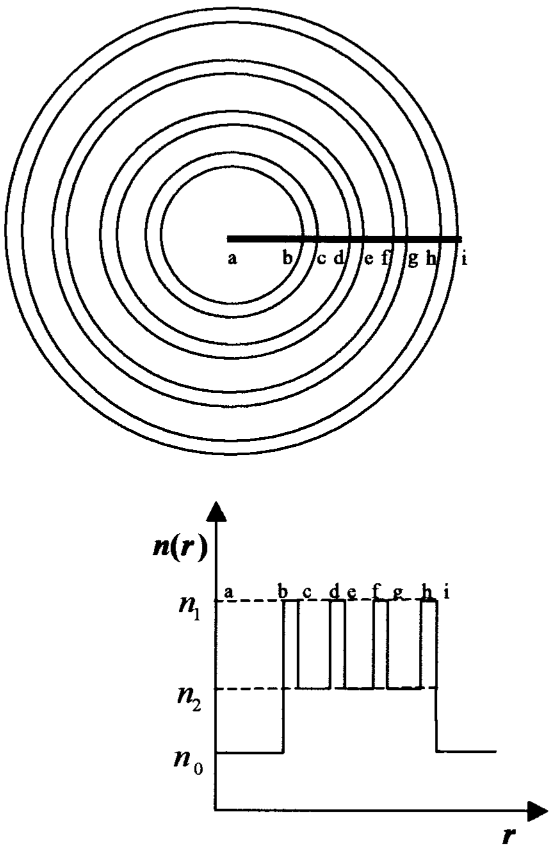

Fig. 1. Cross section of the hollow waveguide showing the hollow core and the dielectric films, also shown is the index of refraction profile in the radial direction.

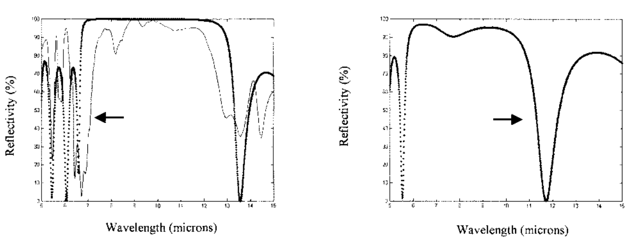

(a) (b)

Fig. 2. (a) Measured (dashed) and calculated (dots) normal incidence reflectance for hollow waveguide in the radial direction. (b) Calculated grazing incidence reflectance for the TM mode.

well as the layer thickness were monitored by IR spectroscopy. The reflectivity of the deposited structure was measured in the radial direction using a Nicolet FTIR microscope and a variable size aperture, to ensure domination by radial reflection. The coated capillary tube was then inserted in a heat shrink tube which was filled with silicone rubber. Finally, the glass tube was dissolved using concentrated hydrofluoric acid (48%). The resulting hollow tube assembly is thus lined with the mirror coating and is both flexible and mechanically stable.

IV. Results and Discussion

The reflectance measurements and simulations are shown for normal incidence in Fig. 2(a). The measured gap width is smaller than predicted, probably due to microdefects in the Te

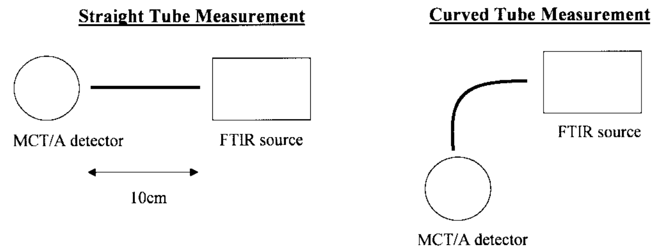

Fig. 3. Hollow tube transmission measurement setup on the spectrophotometer (FTIR).

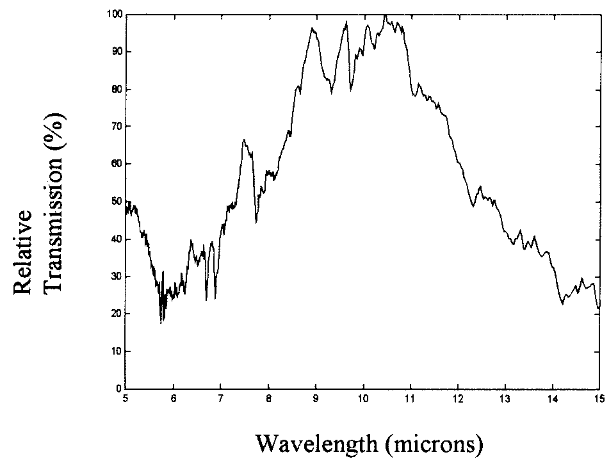

Fig. 4. Transmission through the hollow waveguide around a 90° bend as a function of wavelength.

layers. In addition there are absorption (8 μm) peaks due to the polyurethane. Fig. 2(b) is the calculation of the reflectance at grazing incidence for the TM mode. Since the omnidirectional frequency range is defined from above (high frequency edge) by the normal incidence gap edge (arrow) and from below by the grazing incidence gap edge (arrow) the extent of the gap is completely defined by these two data points. The extent of the omnidirectional range for the parameters used in this experiment is approximately 40% [1], [2].

The transmission through the tube was measured using a Nicolet Magna 860 FTIR bench with an MCT/A detector. The transmission was measured around a 90° bend at a radius of curvature of approximately 1 cm, which was compared, to the straight tube transmission to correct for entrance and exit effects. A schematic of the measurement layout is presented in Fig. 3.

The results shown in Fig. 4 indicate a high transmission around the 90° bend for a spectral band that corresponds to the omnidirectional gap. The relatively high noise level in the measurement is due to the lack of purge. This measurement provides a proof-of-concept indicating the low loss characteristics and guiding abilities of the all dielectric hollow waveguide.

Acknowledgment

The authors would like to thank T. McClure for valuable assistance in the optical setup. This work made use of the National Science Foundation Shared Experimental Analytical Facility.

REFERENCES

[1] J. N. Winn, Y. Fink, S. Fan, and J. D. Joannopoulos, "Omnidirectional reflection from a one-dimensional photonic crystal," *Opt. Lett.,* vol. 23, no. 20, pp. 1573–1575, 1998.

[2] Y. Fink, J. N. Winn, S. Fan, J. Michel, C. Chen, J. D. Joannopoulos, and E. L. Thomas, "An omnidirectional dielectric reflector," *Science,* vol. 282, pp. 1679–1682, 1998.

[3] D. N. Chigrin, A. V. Lavvrinenko, D. A. Yarotsky, and S. V. Gaponenko, "Observation of total omnidirectional reflection from a one-dimensional dielectric lattice," *Appl. Phy. A,* vol. 68, pp. 25–28, 1999.

[4] P. S. J. Russell, S. Tredwell, and P. J. Roberts, "Full photonic bandgaps and spontaneous emission control in 1D multilayer dielectric structures," *Opt. Commun.,* vol. 160, no. 1–3, pp. 66–71, 1999.

[5] M. Miyagi, A. Hongo, Y. Aizawa, and S. Kawakami, "Fabrication of germanium-coated nickel hollow waveguides for infrared transmission," *Appl. Phys. Lett.,* vol. 43, pp. 430–432, 1983.

[6] N. Croitoru, J. Dror, and I. Gannot, "Characterization of hollow fibers for the transmission of infrared radiation," *Appl. Opt.,* vol. 29, pp. 1805–1809, 1990.

[7] Y. Matsuura and J. Harrington, "Hollow glass waveguides with three-layer dielectric coating fabricated by chemical vapor deposition," *J. Opt. Soc. Amer.,* vol. 14, no. 6, 1997.

[8] M. Miyagi and S. Kawakami, "Design theory of dielectric coated circular metallic waveguides for infrared transmission," *J. Lightwave Technol.,* vol. LT-2, pp. 116–126, 1984.

[9] P. Yeh, A. Yariv, and E. Marom, "Theory of a Bragg fiber," *J. Opt. Soc. Amer.,* vol. 68, no. 9, 1978.

Yoel Fink, photograph and biography not available at the time of publication.

Daniel J. Ripin, photograph and biography not available at the time of publication.

Shanhui Fan, photograph and biography not available at the time of publication.

Chiping Chen, photograph and biography not available at the time of publication.

John D. Joannopoulos, photograph and biography not available at the time of publication.

Edwin L. Thomas, photograph and biography not available at the time of publication.